

**Purdue University**  
**Purdue e-Pubs**

---

International Compressor Engineering Conference

School of Mechanical Engineering

---

2016

# Experimental Investigation on the Operating Characteristics of a Semi-hermetic Twin Screw Refrigeration Compressor by means of p-V Diagram

Xiaokun Wu

*Xi'an Jiaotong University, wxiaokun@foxmail.com*

Zhaorui Zhao

*Xi'an Jiaotong University, smile90613@163.com*

Wenqing Chen

*Suzhou Academy, Xi'an Jiaotong University, wqchen\_xjtusz@126.com*

Ziwen Xing

*Xi'an Jiaotong University, zwxing@mail.xjtu.edu.cn*

Follow this and additional works at: <https://docs.lib.purdue.edu/icec>

---

Wu, Xiaokun; Zhao, Zhaorui; Chen, Wenqing; and Xing, Ziwen, "Experimental Investigation on the Operating Characteristics of a Semi-hermetic Twin Screw Refrigeration Compressor by means of p-V Diagram" (2016). *International Compressor Engineering Conference*. Paper 2402.  
<https://docs.lib.purdue.edu/icec/2402>

This document has been made available through Purdue e-Pubs, a service of the Purdue University Libraries. Please contact [epubs@purdue.edu](mailto:epubs@purdue.edu) for additional information.

Complete proceedings may be acquired in print and on CD-ROM directly from the Ray W. Herrick Laboratories at <https://engineering.purdue.edu/Herrick/Events/orderlit.html>

## Experimental investigation on the operating characteristics of a semi-hermetic twin screw refrigeration compressor by means of $p$ - $V$ diagram

Xiaokun Wu<sup>1\*</sup>, Zhaorui Zhao<sup>1</sup>, Wenqing Chen<sup>2</sup>, Ziwen Xing<sup>1</sup>

<sup>1</sup>School of Energy and Power Engineering, Xi'an Jiaotong University,  
Xi'an, Shaanxi, PR China  
(Phone:+86-29-82675258, Fax:+86-29-82663783, E-mail:wxiaokun@foxmail.com)

<sup>2</sup>Suzhou Academy, Xi'an Jiaotong University,  
Suzhou, Jiangsu, PR China  
(Phone:+86-512-69562807, Fax:+86-512-69562807, E-mail:wqchen\_xjtusz@126.com)

\* Corresponding Author

### ABSTRACT

In this paper, a comprehensive experimental investigation is carried out to evaluate the operating characteristics of a semi-hermetic twin screw refrigeration compressor at different oil flow rates and slide valve positions under various conditions. The working volume pressure of the compressor is recorded by a serial of sensors arranged in consecutive positions of the housing. These measured pressure data are then transformed into an indicator diagram. Based on the  $p$ - $V$  diagrams, the effect mechanism of some factors such as evaporation temperature, condensation temperature, slide valve positions, oil flow rates for the suction and discharge end bearings lubricating and oil flow rate returned from the suction pipe on the compressor performance and working process is analyzed. These results can be useful for the optimum design of oil flow passage assembly and selection of optimal built-in volume ratio to improve the energy efficiency of refrigeration system with semi-hermetic twin screw compressor.

### 1. INTRODUCTION

Twin screw compressor is a kind of rotary positive displacement machine, the working cavity of which is enclosed by the housing bores, housing end plates and the helical surfaces of the male and female rotors. With advantages of efficient, reliable and compact, the twin screw compressor has been widely used in industrial refrigeration and central air-conditioning applications [1]. As a key component, the performance of which is very sensitive to a number of design parameters governing the thermodynamic and flow process. Thus the investigation on the operating characteristics of twin screw compressor is of great importance to improving the energy efficiency in refrigeration systems.

The analysis of thermodynamic processes within twin screw compressors by means of indicator diagram is well established and is frequently used as a tool in the design of high efficient compressors. In the case of semi-hermetic twin screw compressor, there are two approaches to access the indicator diagrams. The first is essentially theoretical. In this case a mathematical model is established, following basic thermodynamic laws, which is solved to obtain the performance parameters of the compressor as well as its indicator diagrams [2-5]. The second is essentially experimental. Here the compressor indicator diagrams are obtained from direct measurement and then used to analyze the compressor thermodynamic process. The helical structure of screw compressor is relatively complex and which makes it far more difficult to record the indicator diagrams. In general, in the case of oil-flooded screw compressors, there are two methods for recording indicator diagrams. The first involves the use of a serial of pressure sensors arranged in consecutive positions in the housing so that each is responsible for recording the pressure changes in a certain rotation degree. All the pressure signals are then combined to obtain continuous

pressure data through the whole working cycle[6,7]. Alternatively, one pressure transducer can be embedded into a groove at the root of the female rotor on the discharge side to measure the whole working process [8,9].

In this paper, the working volume pressure of the compressor is recorded by a serial of sensors arranged in consecutive positions in the housing and the characteristics of the compressor is experimentally investigated when operating at different conditions, loads and especially at various lubricating oil flow rates by means of the indicator diagram. Based on the test data, performance parameters, such as the indicated power consumptions, the isentropic indicated efficiency and the mechanical efficiency, are calculated to evaluate the influence of structure and operating parameters on the working process and performance of the semi-hermetic twin screw refrigeration compressor. These results can be useful for optimum design of the compressor to improve the energy efficiency of refrigeration system. Also, the measurement data can supply some guidance for the development of mathematical model used to describe the compressor working process.

## 2. EXPERIMENTAL SET-UP

### 2.1 Modification of the Lubricating Oil Circuit

The lubricating oil circuit of a semi-hermetic twin screw refrigeration compressor is presented in the Figure 1(a). The oil outflowed from sump  $Mo,out$  can be divided into three parts: oil supplied for the suction end bearings  $Mo,s$ , oil supplied for the discharge end bearings  $Mo,d$  and the oil supplied for the capacity regulation  $Mo,l$ . The oil returned from discharge end bearings is then injected into the rotor cavity at the position with built-in volume ratio of 1.1. The oil returned from suction end bearings flows into the rotor cavity along with the intake refrigerant gas. The oil injected machine requires a separator to remove the oil from the high pressure discharged gas. The oil-gas stream from the rotor section exits the inner housing and then directly strikes the filter screens to remove the oil before the refrigerant gas leaves the compressor via the discharge valve. The separated oil is eventually collected in the oil storage sump of compressor assembly. Obviously, a little oil will still exit compressor along with the refrigerant gas because the oil separated efficiency  $\eta$  cannot reach 100%. As a result, additional oil needs to return back to the compressor for maintaining the oil level in the sump. This part of oil usually returns to the suction pipe and flows with refrigerant gas into the compressor. For the purpose of oil flow rate measurement, the screw compressor was modified as shown in Figure 1(b). External oil pipes are used to replace the inner oil loop arranged in compressor housing. Thus, oil flow meters and sight glasses can be installed to measure the oil supplied flow rates for the suction and discharge end bearings. The regulation of oil supplied flow rates are accomplished by the orifice plugs with various diameters and the variations of valves opening.

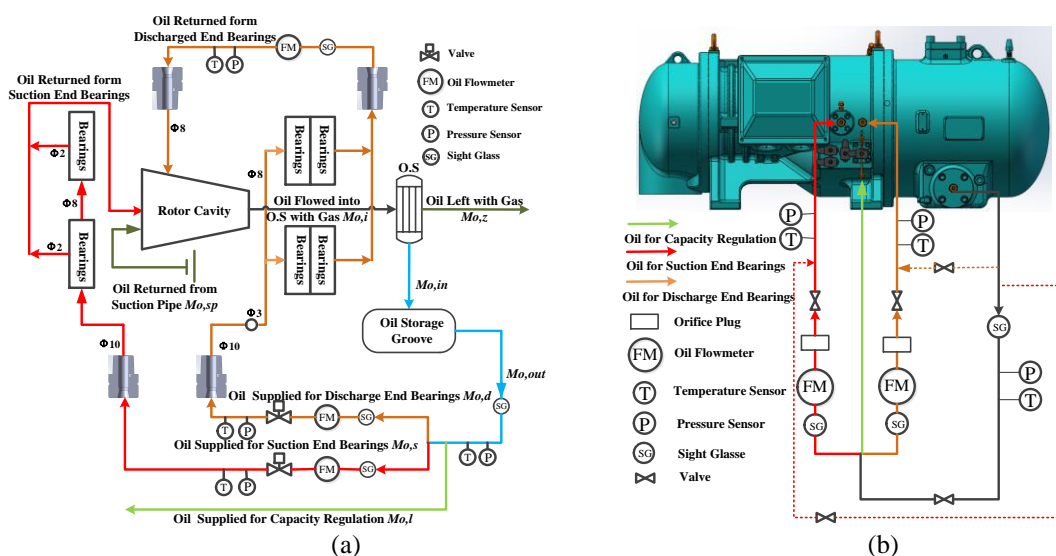
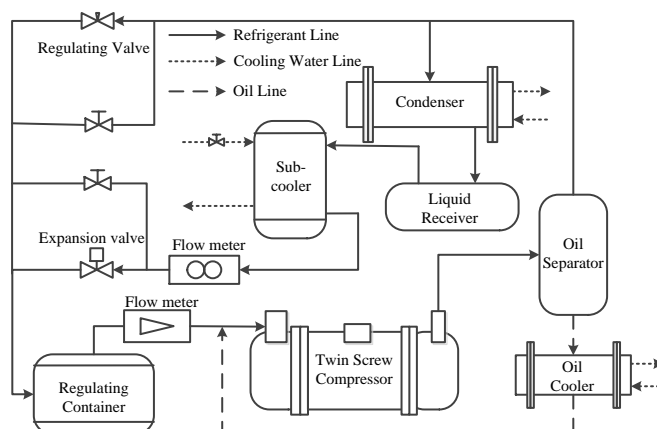


Figure 1 Lubricating oil cyclic system of the screw compressor

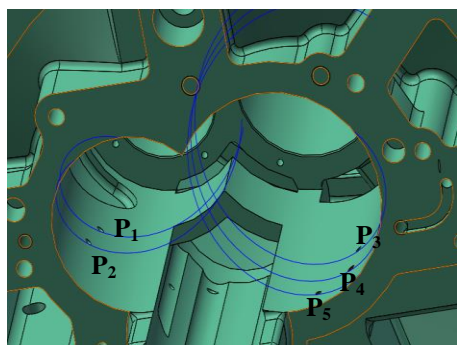
### 2.2 Compressor Test Rig

Performance of the semi-hermetic twin screw refrigeration compressor with built-in volume ratio of 2.4 and R134a as the working fluid under various conditions is measured with the experimental apparatus shown in Figure 2. The gas-oil mixture is compressed in the compressor and discharged into an oil separator. The separated oil is cooled in the oil-cooler and then flows into the suction pipe to return back to the compressor. Part of the high pressure refrigerant gas then enters the condenser, liquid receiver and sub-cooler. The sub-cooled refrigerant liquid flow rate is measured by the Coriolos type mass flow meter. The rest high-pressure refrigerant gas directly flows into a regulating container. The liquid refrigerant from the sub-cooler is throttling. And pressures of the refrigerant gas and liquid are released by the controlling valves. Then heat and mass exchanges sufficiently between refrigerant gas and liquid in the regulating container to the specified low pressure state. The refrigerant flow rate is measured again by a vortex flow meter. Finally, the refrigerant gas flows into the compressor. The data acquisition, processing and archiving are accomplished by a computer and the steady state can be automatically estimated. Simultaneously experimental data is monitored and the working conditions such as the evaporation pressure and condensation pressure can be controlled precisely.

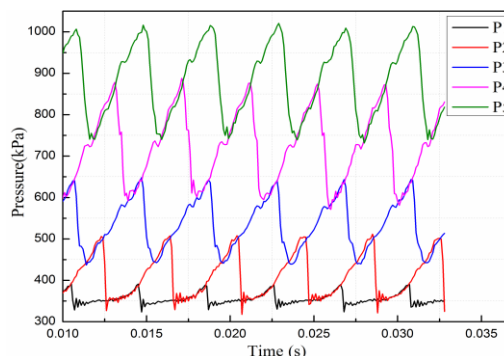


**Figure 2** The screw refrigeration compressor test system

The method for recording indicator diagrams in this paper involves the use of five pressure sensors arranged in consecutive positions in the compressor housing as shown in Figure 3(a). The recording data of the five pressure sensors has a part of overlap and can be used to describe the pressure changes of the suction process, the compression process and part of discharge process. Because there is no position to arrange sensors in the compressor housing, pressure in the rest part of discharge process cannot be measured by this method. So this part of pressure is considered approximately equal to the condensation pressure. The pressure sensors are made by Kulite Group and the model is XTL-140M. The overall error of the sensor is less than  $\pm 0.3\%$  and its response frequency is as high as 10 kHz. The vapor pressure changes along with time in the working chamber named  $p-t$  diagram can be achieved as shown in Figure 3(b) when the compressor operating under  $5^\circ\text{C}/36^\circ\text{C}$  with rotation speed of 2950 r/min and inlet temperature of  $10^\circ\text{C}$ . Then the  $p-t$  diagrams can be transformed to the  $p-V$  diagrams according to the rotation speed and variations of working volume with rotation angles.



(a) Arrangement of pressure sensors



(b)  $p-t$  diagram under  $5^\circ\text{C}/36^\circ\text{C}$

**Figure 3** Installation positions of pressure sensors and the tested  $p-t$  diagram

### 2.3 Performance Parameters

The performance parameters can be calculated from the measured pressures, temperatures, flow rates and the power consumptions. The theoretical volume flow rate  $q_{vt}$  of semi-hermetic twin screw compressor investigated in this paper is  $550 \text{ m}^3/\text{h}$ . Then the volumetric efficiency  $\eta_V$  can be calculated as follows:

$$\eta_V = \frac{q_V}{q_{vt}} \quad (1)$$

The indicated power  $P_{ind}$ , shaft power  $P_{out}$ , isentropic adiabatic power  $P_{ad}$  can also be calculated by the measured data:

$$P_{ind} = z \frac{w}{2\pi} \oint p dV \quad (2)$$

$$P_{out} = P_{in} \eta_m \quad (3)$$

$$\eta_m = -1.027e-07P_{in}^4 + 4.378e-05P_{in}^3 - 0.007P_{in}^2 + 0.488P_{in} + 83.421 \quad (4)$$

$$P_{ad} = q_m (h_{ds} - h_s) \quad (5)$$

Furthermore, the indicated, mechanical, isentropic efficiencies are defined as follows:

$$\eta_{ind} = \frac{P_{ad}}{P_{ind}} \times 100\% \quad (5)$$

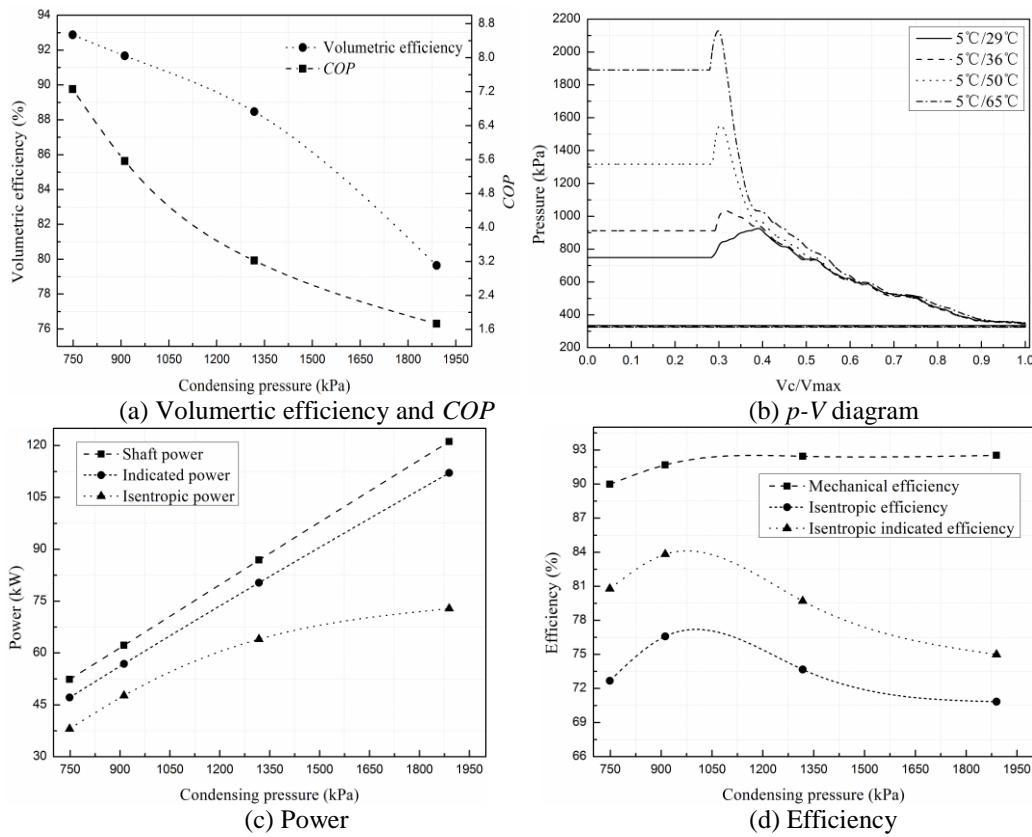
$$\eta_m = \frac{P_{ad}}{P_{out}} \times 100\% \quad (7)$$

$$\eta_{ad} = \frac{P_{ad}}{P_{ind}} \times 100\% \quad (8)$$

## 3. RESULTS AND DISCUSSION

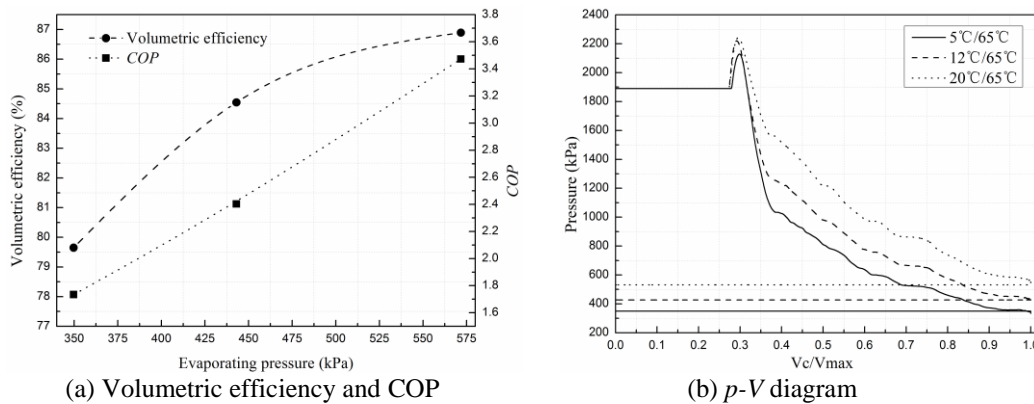
### 3.1 Operating Characteristic at Various Conditions

Figure 4 shows the measured performance parameters and  $p$ - $V$  diagrams of the screw compressor under different condensation temperature conditions. As the pressure difference between the condensation and evaporation side increases, external leakages (leaking to the suction pressure) cause the reduction of volumetric efficiency as presented in Figure 4(a). More refrigerant gas from the discharge process will leak into the following enclosed cavity due to the relative larger condensation pressure. The pressure in enclosed working volume will rise up as presented in Figure 4(b), especially for the working volume near to the discharge end. When operating under  $5^\circ\text{C}/50^\circ\text{C}$  and  $5^\circ\text{C}/65^\circ\text{C}$  conditions, the pressure when the working volume connects with discharge port (with built-in volume ratio of 2.4) is smaller than the condensation pressure (under-compression condition), the refrigerant gas under higher pressure will flow reversely to the working chamber and the pressure in working volume will rapidly increase. Moreover, due to the existence of flow resistance during the discharge process, the pressure in discharge process needs to be larger than the condensation pressure so that the normal discharge process can begin. It is similar with the condition of  $5^\circ\text{C}/36^\circ\text{C}$ . The pressure in the discharge process is also large than the condensation pressure even though the pressure when working volume is open to the discharge port is nearly to the condensation pressure in this condition. When operating under  $5^\circ\text{C}/29^\circ\text{C}$ , the pressure when the working volume is open to the discharge port is larger than the condensation pressure (over-compression condition), the pressure drops as the discharge area increases. As the pressure line rises in the  $p$ - $V$  diagrams, the indicated power and shaft power consumption of screw compressor increase. The isentropic power is also larger but the amplification is gradually to be slow down because the suction volume flow rate reduces as presented in Figure 4(c). Figure 4(d) gives the variation of efficiency of the screw compressor under different condensation temperature conditions. There exists an optimal operating condition for the isentropic and indicated isentropic efficiency. And under this condition the built-in compression end pressure is nearly equal to the condensation pressure. Moreover, the mechanical efficiency increases with the condensation temperature. It implies that the indicated power proportion of shaft power will continuously rise as the increase of condensation temperature.



**Figure 4** Performance parameters and  $p$ - $V$  diagrams under different condensing temperature

Figure 5 gives the performance parameters and  $p$ - $V$  diagrams under different evaporation temperature. It can be observed that the volumetric efficiency increases as the evaporating pressure rises up due to the reduction of pressure difference through the external leakage paths. The pressure of compression process described in the  $p$ - $V$  diagram ascends because the beginning pressure of the whole compression process increases with the evaporation pressure. The indicated power consumption calculated by the  $p$ - $V$  diagram correspondingly increases. The density of R134a in the suction state increases so that the mass flow rate of R134a rises up which results in the increase of isentropic power even though the difference pressure between the evaporation and condensation reduces. The built-in compression end pressure is always smaller than the condensation pressure in the three testing conditions. However, the degree of under-compression is alleviated with the ascend of evaporation pressure which is beneficial to the isentropic and isentropic indicated efficiency as shown in Figure 5(d). Moreover, the mechanical efficiency is also increased with the evaporation pressure which is similar with the condition of condensation pressure increase.



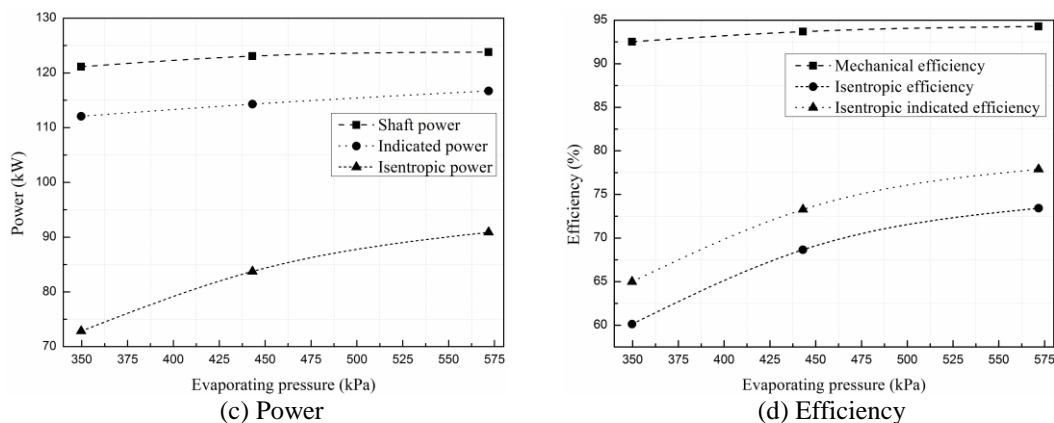


Figure 5 Performance parameters and  $p$ - $V$  diagrams under different evaporating temperature

### 3.2 Operating Characteristic at Different Loads

Figure 6 shows the performance parameters and  $p$ - $V$  diagrams under different loads with an evaporation temperature of  $5^{\circ}\text{C}$  and a condensation temperature of  $36^{\circ}\text{C}$ . It can be observed that both the cooling capacity and the COP decrease as the load drops in Figure 6(a). That is due to the mechanism for slide valve to achieve capacity control. When the slide valve contacts with the slide stop to keep a seal between them, the compressor is under the full load condition. The R134a gas is drawn in by the rotation of the rotors, trapped between the rotors and the casing, compressed as the rotors meshed each other. When a by-pass port appears due to the movement of the slide valve, the compressor is under part-load condition. As soon as the rotors start to mesh and try to increase the gas pressure, the working volume exposes to the suction pressure through the by-pass port. Gas pressure rise in the working volume is slowed down, even held under the suction pressure until the contact line moves to the end of the by-pass port due to some gas venting back to the low pressure cavity, thereafter the working chamber is enclosed and the normal compression begins as shown in the  $p$ - $V$  diagram of Figure 6(b).

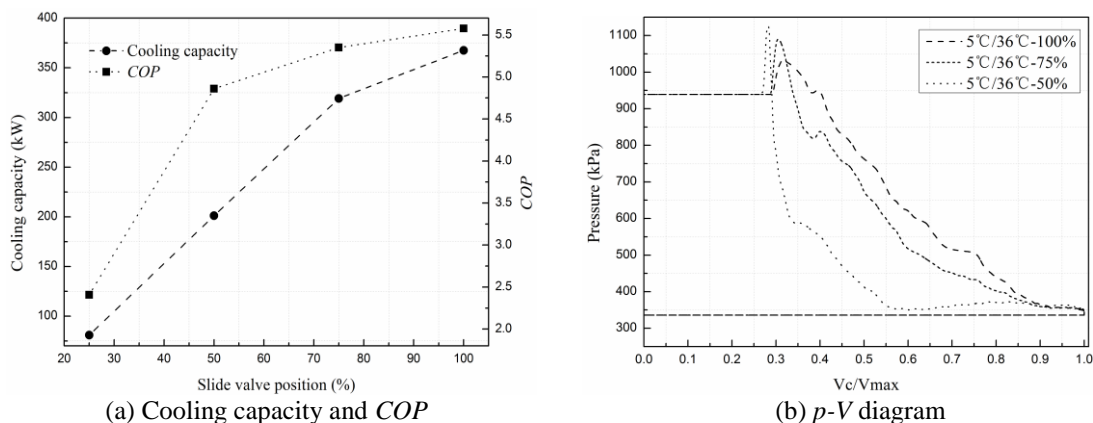


Figure 6 Performance parameters and  $p$ - $V$  diagram under different loads

### 3.3 Operating Characteristic under Various Oil Cyclic Flow Rates

For the purpose of maintaining the oil level in the sump, additional oil needs to compensate into the compressor and this part of oil usually returns to the suction pipe. Figure 7 gives the performance parameters and  $p$ - $V$  diagrams with different oil return flow rates from suction pipe  $M_{o,sp}$ . The volumetric efficiency and COP reduce as the  $M_{o,sp}$  increases. That is because that this part of oil flows along with gas from the suction valve and then is drawn in with gas by the rotation of rotors. As a result, part of the enclosed working volume is occupied by the oil. Moreover, the increase of oil flow rate causes extra flow resistance when gas-oil mixture flowed through the motor cavity which is detrimental to the volumetric efficiency. The pressure at the compression beginning position is also reduced with the increase of  $M_{o,sp}$  as shown in the Figure 7(b). The higher volumetric efficiency means larger gas mass in the working volume which will cause higher working volume pressure as the reduction of oil flow rate. Another reason for increase of working volume pressure is the cooling effect of oil. This part of oil is firstly cooled in an oil-cooler



installed at the test rig system to temperature of almost 20°C. In the compression process, this part of oil can absorb a certain amount of heat from refrigerant gas which causes the decline of pressure line in  $p$ - $V$  diagram. Correspondingly, the indicated power calculated by the  $p$ - $V$  diagram is larger as the oil flow rate increases as shown in Figure 7(c). The shaft power consumption also increases but the augment rate is small. That is because the increase of oil flow rate entering the rotor cavity which will alleviate the friction power loss to a certain degree. As a result, the mechanical efficiency is increased as shown in Figure 7(d). The isentropic power decreases with the increase of oil flow rate due to the reduction of gas volume flow rate. So the isentropic and isentropic indicated efficiency also reduce as the oil flow rate increases which implies that the increase of oil flow return flow rate from the suction pipe has adversely effect on the performance of screw compressor.

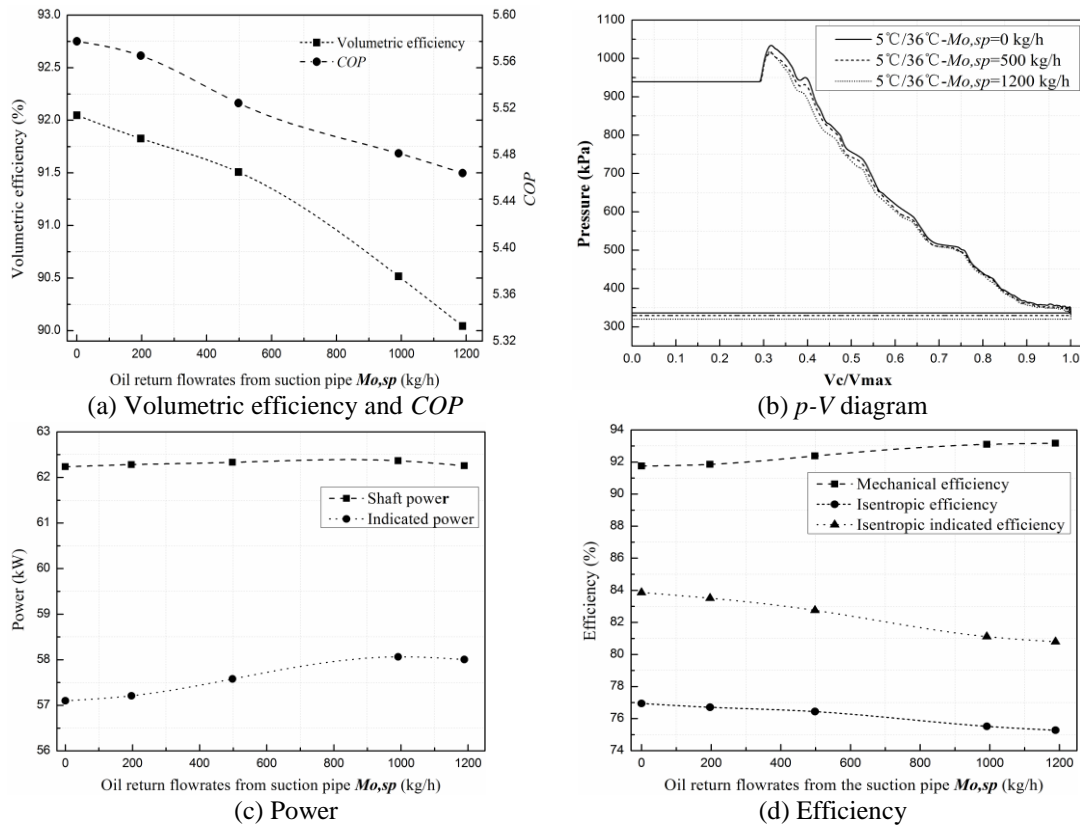
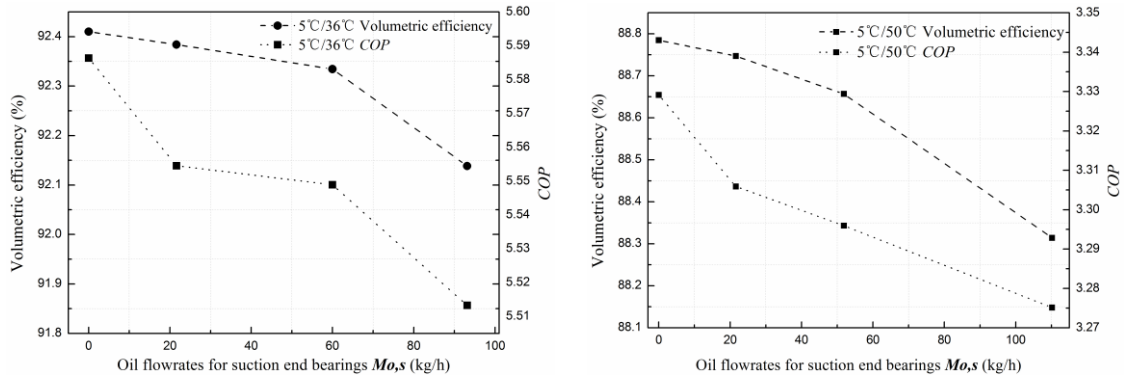


**Figure 7** Performance parameters and  $p$ - $V$  diagrams under different oil return flow rates from suction pipe

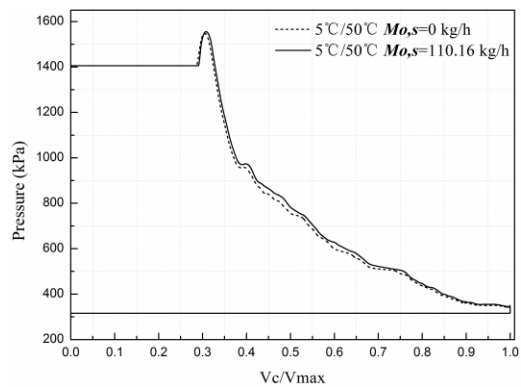
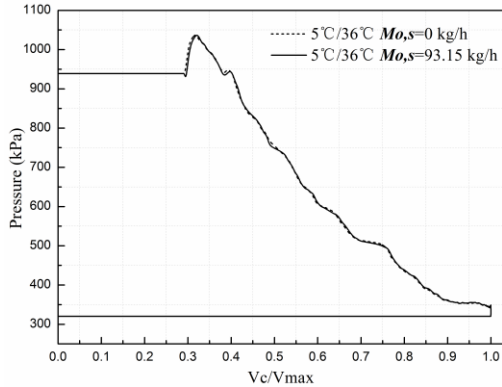
Performance parameters and  $p$ - $V$  diagrams at different oil flow rates for suction end bearings under conditions of 5°C/36°C and 5°C/50°C are shown in Figure 8. The oil flow rates are adjusted by replacement of orifice plugs installed in the oil supplied pipe. As the oil flow rates increase from zero to the maximum value, the volumetric efficiency reduces slightly. That is mainly because that the oil flows along with refrigerant gas into the working volume which is still at suction process, the oil will occupy part of working volume. Figure 8(c) and (d) give the  $p$ - $V$  diagram at different oil flow rate. It can be observed that the pressure line with larger oil flow rate is higher than that with smaller oil flow rate. That is because that the oil temperature for suction end bearings lubricating is from the sump of discharge housing where the temperature is nearly to the discharge temperature. Once such high temperature oil enters the working volume, the gas should be heated and gas pressure will increase. The larger amount of oil with higher temperature enters into the working volume, the higher of gas pressure would be. That is why the increase rate of pressure when operating at 5°C/50°C is larger compared with the condition of 5°C/36°C. The indicated power consumption calculated by the  $p$ - $V$  diagram and the shaft power are also increased as shown in Figure 8(e) and (f). The isentropic power reduces due to the reduction of refrigerant volume flow rate. As a result, the isentropic and isentropic indicated efficiency also decline with the increase of oil flow rate as shown in Figure 8(g) and (h). The friction energy loss of suction end bearings is alleviated as the oil flow rate increasing. Thus, the mechanical efficiency increases.





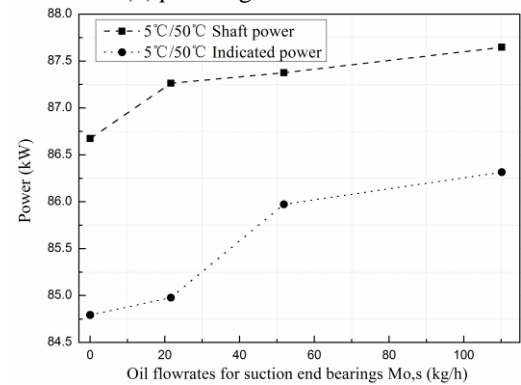
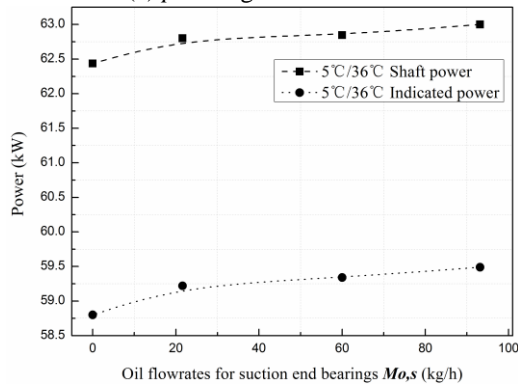
(a) Volumetric efficiency and COP under 5°C/36°C

(b) Volumetric efficiency and COP under 5°C/50°C



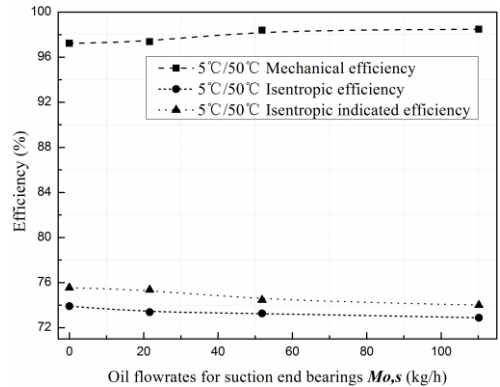
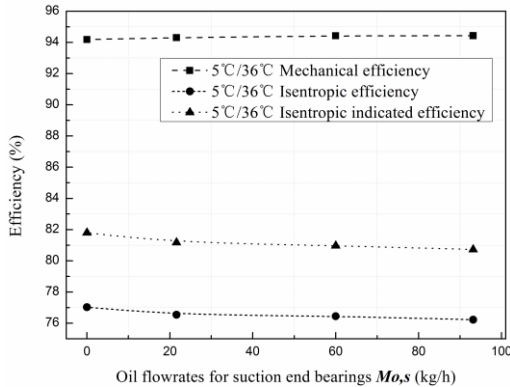
(c)  $p$ - $V$  diagram under 5°C/36°C

(d)  $p$ - $V$  diagram under 5°C/50°C



(e) Power under 5°C/36°C

(f) Power under 5°C/50°C

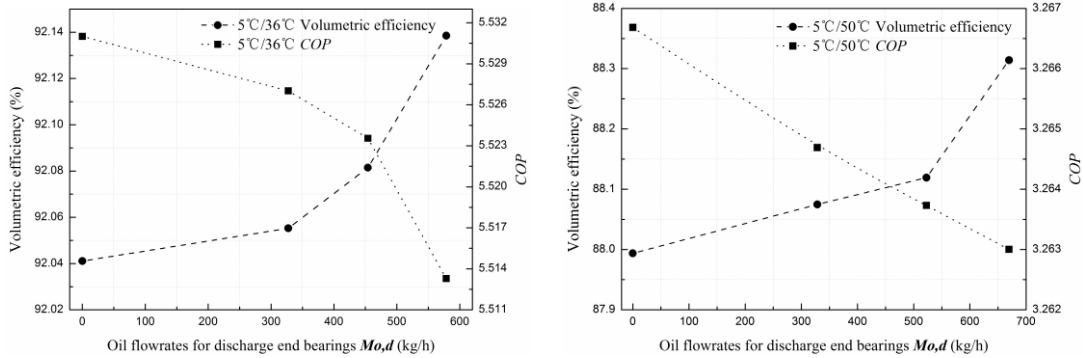


(g) Efficiency under 5°C/36°C

(h) Efficiency under 5°C/50°C

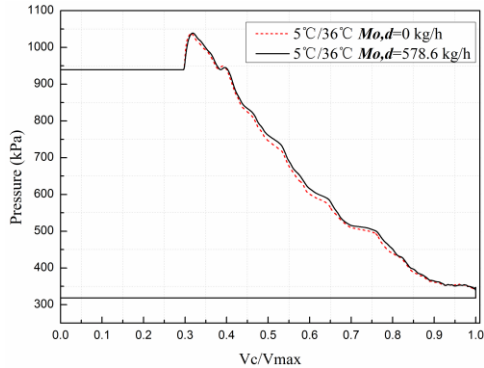
Figure 8 Performance parameters and  $p$ - $V$  diagrams under different oil flow rates for suction end bearings

Performance parameters and  $p$ - $V$  diagrams at different oil flow rates for discharge end bearings lubricating under conditions of  $5^{\circ}\text{C}/36^{\circ}\text{C}$  and  $5^{\circ}\text{C}/50^{\circ}\text{C}$  are shown in Figure 9. As the oil flow rate rises from zero to the maximum, the volumetric efficiency slightly increases. Different from the oil for suction end bearings lubricating, the oil for discharge end bearings returns to the working volume which has already enclosed. The oil will not occupy the working volume and this part of oil entering into the rotor cavity has a favorable effect on the sealing of leakage paths. However, the promote range is slight as the oil flow rate increases. It indicates that the oil flow rate coming from the suction pipe and suction end bearings is enough for the leakage path sealing effect. Extra oil flowing into the rotor cavity from the discharge end bearings has little promote effect on the volumetric efficiency. However, the pressure of working volume rises up with increase of the oil flow rate as shown in Figure 9(c) and (d). Similar with the oil for suction end bearings lubricating, the temperature of oil for discharge end bearings is also nearly equal to the discharge temperature. Once this part of oil flows into the rotor cavity, the gas of the working volume will be heated by the high temperature oil and correspondingly the pressure will increase. The indicated power calculated from the  $p$ - $V$  diagram and the shaft power rise as the oil flow rate increase as shown in Figure 9(e) and (f). The mechanical efficiency has a slightly increase due to the reduction of friction loss of the discharge end bearings. And the isentropic indicated efficiency reduces which implies that additional oil entering from the discharge end bearings has an adverse effect on the screw performance once the oil flow rate entering into the rotor cavity is enough for the sealing of leakage paths.

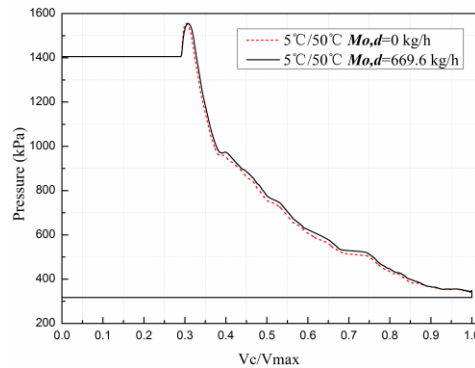


(a) Volumetric efficiency and COP under  $5^{\circ}\text{C}/36^{\circ}\text{C}$

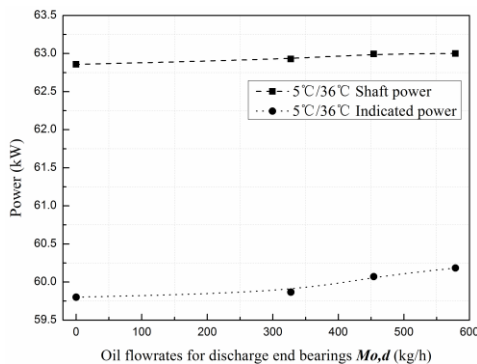
(b) Volumetric efficiency and COP under  $5^{\circ}\text{C}/50^{\circ}\text{C}$



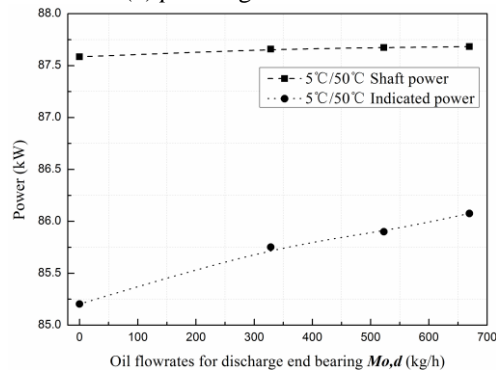
(c)  $p$ - $V$  diagram under  $5^{\circ}\text{C}/36^{\circ}\text{C}$



(d)  $p$ - $V$  diagram under  $5^{\circ}\text{C}/50^{\circ}\text{C}$



(e) Power under  $5^{\circ}\text{C}/36^{\circ}\text{C}$



(f) Power under  $5^{\circ}\text{C}/50^{\circ}\text{C}$

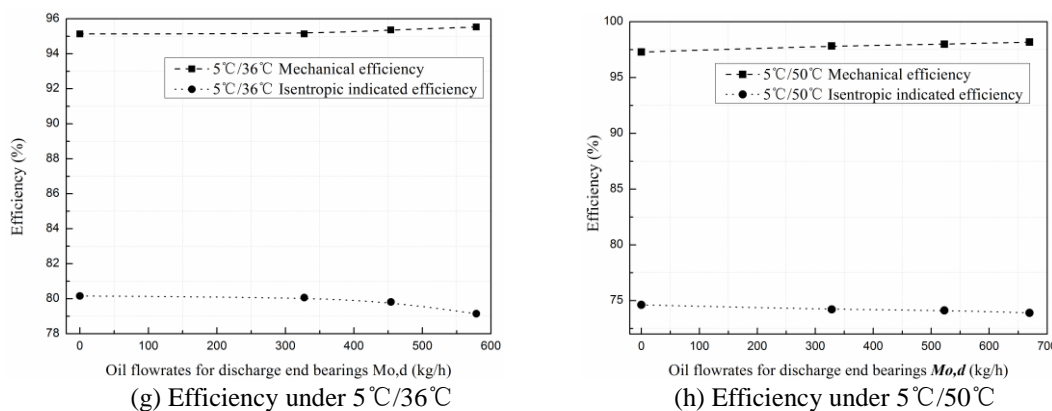


**Figure 9** Performance parameters and  $p$ - $V$  diagrams under different oil flow rates for discharge end bearings

Figure 10 gives the volumetric efficiency when different oil flow rates enter into the rotor cavity. This part of oil consists of the oil for suction and discharge end bearing lubricating and the returned oil from the suction pipe. The volumetric efficiency firstly rises up with the increase of this part oil due to the sealing effect of oil on the leakage paths. Then the increase rate becomes slight which indicates that the oil for sealing is enough. The reason why the volumetric efficiency eventually descends is because that in this stage the increase of oil entering into the rotor cavity is mainly caused by the increase of oil returned from the suction pipe which has an adverse effect on the volumetric efficiency. The minimum oil flow rate for sealing of leakage paths can be accessed. For the condition of  $5^{\circ}\text{C}/36^{\circ}\text{C}$ , the minimum oil flow rate is 677.45 kg/h, the volume ratio of oil and gas is 0.15%. As for the condition of  $5^{\circ}\text{C}/50^{\circ}\text{C}$ , the minimum oil flow rate needed for sealing is larger than the condition of  $5^{\circ}\text{C}/36^{\circ}\text{C}$  due to the larger pressure difference through the leakage paths and the minimum oil flow rate reaches 1334.51 kg/h, the corresponding oil-gas volume ratio is 0.3%.

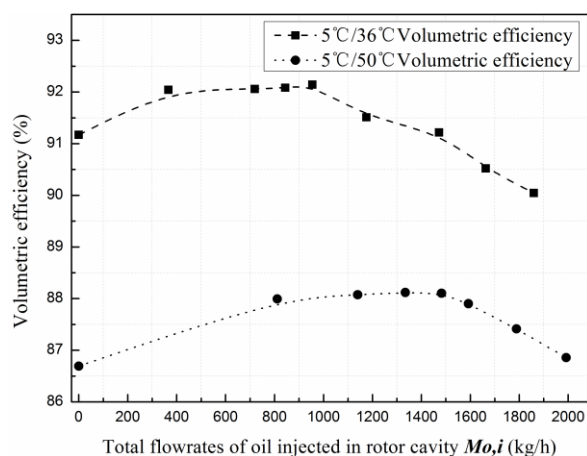


**Figure 10** Volumetric efficiency at different oil flow rates entering into the rotor cavity

#### 4. CONCLUSIONS

A comprehensive experimental investigation is carried out to evaluate the operating characteristic of a semi-hermetic twin screw refrigeration compressor under various conditions. The  $p$ - $V$  diagram is also recorded to analyze the internal working process. The effects of operating conditions, slide valve positions and oil flow rates on the performance parameters are evaluated. The following conclusions are obtained from the results of the investigation:

- As the condensation temperature increases, the pressure line in the  $p$ - $V$  diagram rises up. The shaft power, indicated power and isentropic power of the twin screw compressor increase while volumetric efficiency and the  $COP$  decrease. Isentropic efficiency and isentropic indicated efficiency reach the highest when the internal pressure ratio is matching with the external pressure ratio.
- When operating under part-load, an obvious pre-compression process and pressure reduction process exist in the  $p$ - $V$  diagram recorded. As the slide valve position increases, the cooling capacity and  $COP$  increase.

- As the oil flow rate returned from suction pipe increases, the pressure line in the  $p$ - $V$  diagram declines. The shaft power, indicated power and mechanical efficiency increase while the volumetric efficiency, isentropic efficiency, isentropic indicated efficiency and COP decrease.
- As the oil flow rate for suction end bearings lubricating increases, the pressure line in the  $p$ - $V$  diagram slightly rises. The shaft power, indicated power and the mechanical efficiency increase while the volumetric efficiency, isentropic efficiency, isentropic indicated efficiency and COP decrease.
- As the oil flow rate for discharge end bearings lubricating increases, the pressure line in the  $p$ - $V$  diagram rises. The shaft power, indicated power and the volumetric efficiency increase while the mechanical efficiency, isentropic indicated efficiency and the COP decrease.
- There exists a minimum oil flow rate for the sealing of leakage paths in the rotor cavity. The optimal volume ratio of oil and gas is 0.15% for condition of 5/36°C and 0.3% for condition of 5/50°C.

## NOMENCLATURE

$\eta$	efficiency	(-)
$q_v$	volume flow rate	(m <sup>3</sup> /h)
$q_m$	mass flow rate	(kg/s)
$P$	power	(kW)
$h$	specific enthalpy	(kJ/kg)
<b>Subscript</b>		
ind	indicated	
ad	adiabatic	
m	motor	

## REFERENCES

- [1]. Z.W. Xing, Screw compressors: Theory, design and application. *China Machine Press*, 2000(In Chinese).
- [2]. Stosic N, Milutinovic L, Hanjalic K and Kovacevic A, Investigation of the influence of oil injection upon the compressor working process, *Int.J.Refrig*, 1992,15(4),355-219.
- [3]. Fleming J.S and Tang Y, The analysis of leakage in a twin screw compressor and its application to performance improvement. *Proc. Instn Mech. Engrs, Part C: J. Mechanical Engineering Science*, 1995, 212(5), 125-136.
- [4]. H.G. Wu, Z.W. Xing, P.C. Shu, Theoretical and experimental study on indicator diagram of twin screw refrigeration compressor, *International Journal of Refrigeration* 27 (2004) 331-338.
- [5]. W.Q. Chen, Z.W. Xing, H. Tang, H.G. Wu, Theoretical and experimental investigation on the performance of screw refrigeration compressor under part-load conditions, *International Journal of Refrigeration* 34(2011) 1141-1150.
- [6]. J.B. Shen, H. Tang, Z. Zhang, Z.W. Xing, Experimental study of a water injected twin screw compressor for mechanical vapor compression system. *International Compressor Engineering Conference at Purdue, USA*, 2014.
- [7]. Haugland K et al, Pressure indication of twin screw compressor. *Proc.10<sup>th</sup> International Compressor Engineering Conference at Purdue, USA*, pp. 450-456, 1990.
- [8]. X.Y. Peng, Z.W. Xing, T.S. Cui, L.S. Li, Analysis of the working process in an oil-flooded screw compressor by means of an indicator diagram. *Proc. Instn Mech. Engrs, Part A: J. Power and Energy*, 2002, 465-470.
- [9]. H.G. Wu, J.F. Li, Z.W. Xing, Theoretical and experimental research on the working process of screw refrigeration compressor under superfeed condition, *International Journal of Refrigeration* 30 (2007) 1329-1335.

## ACKNOWLEDGEMENT

The authors would like to acknowledge the financial support from the National Nature Science Foundation of China (Grant No.51276134) and the National Nature Science Foundation of Jiangsu province of China (Grant No.BK20150380).